SPWLA 38th Annual Logging Symposium, June 15-18, 1997

Real Time Interpretation of MWD Anisotropy in High Angle Wells, Offshore Gulf of Mexico

Victor Rosato, Spirit Energy 76, Lafayette, Louisiana
Joseph Beck, Sperry-Sun Drilling Services, Lafayette, Louisiana

ABSTRACT

The purpose of this article is to tabulate the range of anisotropy observed on real time MWD logs, offshore Gulf of Mexico, in order to aid in the interpretation of the data. A table is presented which includes age, depositional environment, and anisotropy ratios, at various relative dip angles. Log examples and their models are also presented. The table can be used to predict the anisotropy ratio a formation may exhibit.

Anisotropy is a condition where sensors exhibit different results when measuring a unit volume from different directions. This effect has been observed on numerous real time MWD logs with high relative dip angles. Predicting anisotropy effects in a formation can be extremely important in determining zone tops and geosteering within the objective zone at high relative dip angles.

There is not an easy way to predict the anisotropy ratio (Rv/Rh) without a high relative dip angle hole, extensive core analysis, or forward modeling. In older fields without modern logs or core material, pre-drill models require numerous assumptions. References cite observed Rv/Rh ratios as great as 50 to 1 (Lesso and Kashikar, 1996). A rule of thumb for pre-drill models in low resistivity pay zones is to begin with ratios of 3 for shales and 1 for sands. In higher resistivity pay zones, a ratio of 2 for shales and 6 for sands is used. Observed anisotropic effects vary by field, formation age, depositional environment, depth of investigation, and apparent dip angle.

INTRODUCTION

The number of high angle wells drilled has increased tremendously as operators discovered their economic benefits. These wells require real-time MWD interpretation for optimum well placement. Often the MWD interpretation is not straightforward due to resistivity anisotropy (Anderson, et al., 1994), which is a condition where the electrical sensors exhibit different results when measuring a unit volume from different directions (Lesso and Kashikar, 1996). Depending on the anisotropy ratio (Rv/Rh), it can be difficult in real-time situations to determine lithology and to stay within the target zone.

Some real-time questions are: Does an increase in resistivity represent an approaching bed, or is it an anisotropy effect in a single lithology as relative dip angle increases? Does the separation in resistivity curves represent invasion, or is it the result of various tool spacings? Is there a gamma ray anisotropy affect? How does varying water saturation affect tool response, and what is the response in a water-bearing sand?

To aid with interpretation, a table of data was assembled from offshore Gulf of Mexico wells. Target zones included Pliocene to Miocene sandstones, from 4,500' to 12,800' TVD, containing gas and/or oil. The working hypothesis was that low-resistivity, low-contrast sands exhibit low anisotropy ratios with high ratios in the adjacent shales. Higher resistivity, high contrast sands should exhibit high anisotropy ratios with low ratios in the adjacent shales.

The general anisotropy signature of the EWR Phase-4™ tool in shale formations is a slight separation between the extra shallow and shallow curves, larger separation between the shallow and medium curves, and the medium and deep curves are approximately equal (Bittar and Rodney, 1996). All MWD examples shown are from phase resistivity measurements. Other factors besides anisotropy that can cause the phase measurements to separate are hole rugosity, borehole effects, invasion, and bed boundary proximity (Bittar, et al., 1991). Invasion and borehole effects are assumed minor since formation exposure time is normally short and hole size is generally in gauge.

The relative dip angle (RDA) is defined as the angle between the well bore and a vector normal to the bedding plane.

The anisotrophy ratio is defined as the ratio of Rv/Rh from the deep reading sensor (SEDP). Rv is the true

resistivity in a vertical plane, as when the tool is parallel to bedding. Rh is the resistivity value measured in a horizontal plane, as when the tool is perpendicular to bedding (Bittar, et al., 1991). Rh values are from RDA's less than 60 degrees. These values came from pilot holes, near-by wells, or the build section of the well. Rh values are from RDA's greater than 70 degrees.

Predrill models are successful in anticipating log responses. Model inputs include well path, bed boundaries, Rv and Rh for each bed, formation dip and direction.

For most horizontal well projects the procedure is: 1) model the pilot hole/offset log, 2) model horizontal well using reasonable assumptions for Rv/Rh, and 3) drill and evaluate horizontal well.

OBSERVATIONS AND DISCUSSION

Table 1 lists the resistivity values at various RDA's for seven offshore Gulf of Mexico fields. Depths range from 4,900' to 12,800' TVD. Ages are from Pliocene to Miocene for various depositional environments. Each field has several data sets, separated by blank rows, which represent the same bed at various RDA's. The data is from pilot, offset, and/or horizontal wells. All wells were drilled with similar water-based drilling fluids. Additional data will be added as more wells are released.

Two primary well types were observed and will be denoted as Type I and II.

Type I wells at low RDA's exhibit low resistivity in shales, with little or no separation of resistivity curves, and high resistivity in hydrocarbon-bearing sands. At high RDA's, shales of Type I exhibit little or no increase in the anisotropy ratio (Rv/Rh ≈ 1.3). A possible reason for the lack of anisotropy in some shales may be bioturbation, which may homogenize the shale and destroy laminations. Rv/Rh ratios in hydrocarbon-bearing sands can be high, with values above 10 and resistivities over 200 Ω-m. This may not be attributable to anisotropy, but rather polarization horn effects. Polarization horns are generally at distinctive bed boundaries with high resistive contrasts between beds. Figures 1 to 4 are a pilot hole, forward model, and high RDA sections (real-time and recorded) of a Type I well.

Type I wells are easy to interpret. Sands and shales are distinguishable from the gamma ray response (SGRC). At high RDA's, the resistivity curves detect approaching bed boundaries in order of depth of investigation. In Figures 3 and 4 the deep curve (SHDP) detects the boundary approximately 40' MD before the bed boundary.

Type II wells exhibit low resistivity in both sands and shales at low RDA's. Low resistivity in sands could be due to several reasons, such as clay types, thin laminations, conductive minerals, fine grain size, high bound water, etc. (Boyd, et al., 1994). At high RDA's, some Type II thick shales can show higher resistivities than hydrocarbon-bearing sands, with shale anisotropy ratios as high as 7. In general, low resistivity-low contrast formations exhibit anisotropy ratios about 3 for thick shales and 1.2 for sands at high RDA's. Separation between resistivity curves increases with RDA starting about 65 degrees. Figures 5 to 8 are a nearby vertical well, forward model, and high RDA sections (real-time and recorded) of a Type II well.

Type II wells from laminated sand/shale sections are more difficult to interpret. Polarization horns and anisotropy in the sands are suppressed. The gamma ray is less definitive of lithology type, and thick shales exhibit high resistivity and large curve separation at high RDA's due to anisotropy. However, in thinly laminated sand/shale pay zones at RDA's near 90 degrees, anisotropy effects and curve separation are reduced (Figures 7 and 8). In this situation, bed boundaries are near parallel to the tool and laminations are less than the diameter of investigation.

CONCLUSIONS

Two primary types of well log responses have been seen:

- Type I - normal to high contrast pay zones with high anisotropy ratios, bounded by shales with low anisotropy ratios; and
- Type II - low resistivity low-contrast pay zones bounded by shales with high anisotropy ratios.

Preliminary results suggest that formation age and TVD does not appear to influence anisotropy. When an interlaminated sand/shale sequence was encountered, regardless of depositional environment, the potential

for high anisotropy ratios at high RDA's was increased. Data from deep water depositional environments was not available. Conclusions about these environments can not be made at this time.

In general, anisotropy effects were minimal (Rv/Rh ≈ 1) for RDA's less than 60 degrees. From 60 to about 80 degrees, anisotropy ratios increase to their maximum values. Beyond 80 degrees, anisotropy ratios remain approximately at maximum values. This is more pronounced in Type II wells.

The observed range of anisotropy ratio in Type I shales is 1 to 2. The range in Type II thick shales is 1 to 7. In thinly laminated sand/shale pay zones at RDA's near 90 degrees, anisotropy effects and curve separation are reduced.

After deciding which well type (Type I or II), lithologic boundaries, and anisotropy ratios are expected, a pre-drill model can be constructed which will assist in real-time interpretation of the high angle well.

NOMENCLATURE

EWR Phase4™	Sperry-Sun's electromagnetic wave resistivity tool
FEWD	formation evaluation while drilling
INC	tool inclination
MEDP	modeled phase derived deep resistivity
MEMP	modeled phase derived medium resistivity
MESP	modeled phase derived shallow resistivity
MEXP	modeled phase derived x-shallow resistivity
MD	measured depth
MWD	measurement while drilling
RDA	relative angle between tool and bedding plane
Rh	vertical resistivity
Rv	horizontal resistivity
Rv/Rh	anisotropy ratio
SEDP	phase derived deep resistivity
SEMP	phase derived medium resistivity
SESP	phase derived shallow resistivity
SEXP	phase derived x-shallow resistivity
SGRC	API gamma ray units
TVD	true vertical depth
VD	vertical depth

ACKNOWLEDGMENTS

The authors wish to thank Spirit Energy 76 for release of the well data.

REFERENCES

Anderson, B., Bryant, I.,Helbig, K., Lilling, M., and Spies, B., 1994, "Oilfield Anisotropy: Its Origins and Electrical Characteristics". Oilfield Review, October pp. 48-55.

Bittar, M., and Rodney, P., 1996, "The Effects of Rock Anisotropy on MWD Electromagnetic Wave Resistivity Sensors". The Log Analyst, vol. 37, no. 1, pp. 20-30.

Bittar, M., Rodney, P., Mack, S., and Bartel, R., 1991, "A True Multiple Depth of Investigation Electromagnetic Wave Resistivity Sensor: Theory, Experiment and Field Test Results". SPE Formation Evaluation, Vol. 8, No. 3, pp 300-320.

Boyd, A., Davis, B., Flanm, C., Klien, J., Sneider, R., Sibbit, A., and Singer, J., 1994, "The Lowdown on Low-Resistivity Pay". Oilfield Review, October pp. 4-18.

Lesso, W.G., and Kashikar, S.V., 1996, "The Principles and Procedures of Geosteering". IADC/SPE 35053, pp. 133-145.

AUTHORS

Victor Rosato is a geologist/team leader with Spirit Energy 76. He joined Spirit Energy 76 in 1974 and has been on exploration and development teams in California and Gulf of Mexico. Victor received his BS in geology from University of California at Davis in 1971 and MS, in oceanography from Oregon State University in 1974.

Joseph Beck is a petrophysicist with Sperry-Sun Drilling Services. He joined Sperry-Sun in 1996 and has been working on log analysis and theoretical modeling of MWD propagating electromagnetic wave tools. Joseph received his BS in Geology from Ball State University in 1980 and MS in Mathematics from Sam Houston State University in 1990. Readers may contact Joseph at his e-mail address: jbeck@sperry-sun.com

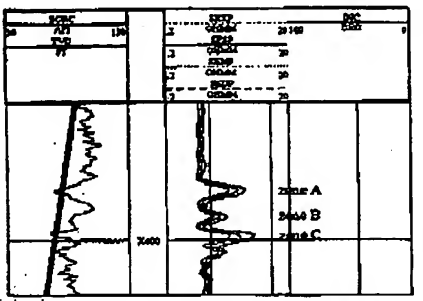

Fig. 1 Type I pilot well, MWD recorded data

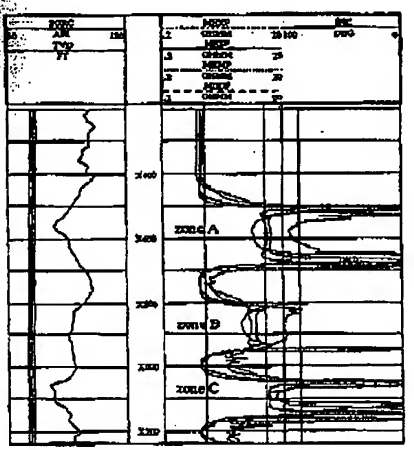

Fig. 2 Type I horizontal forward model
zone Rv/Rh = 6.0 shale Rv/Rh = 1.3
SGRC from pilot well

Note: Pilot and model include zones A, B, and C
and actual well path is in A and B only.

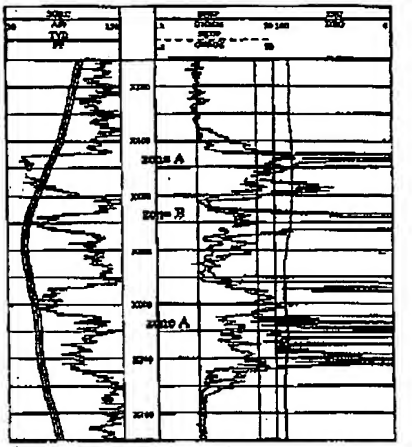

Fig. 3 Type I horizontal well, MWD real time data

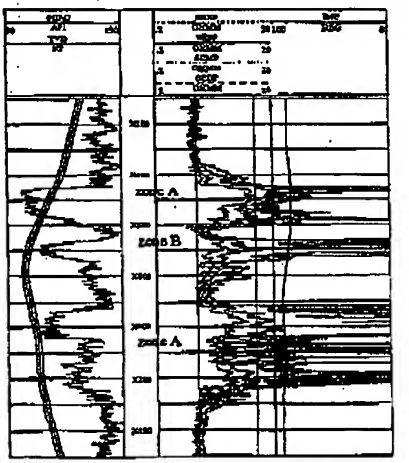

Fig. 4 Type I horizontal well MWD recored data

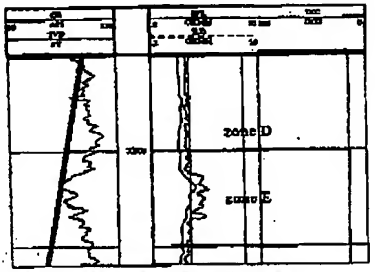

Fig. 5 Type II offset well, wireline data

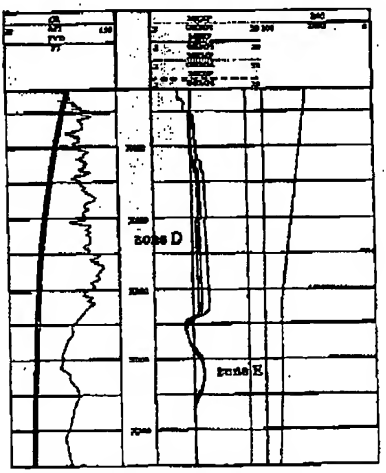

Fig. 6 Type II horizontal forward model
sand Rv/Rh = 1.1 shale Rv/Rh = 3.0
GR from offset well

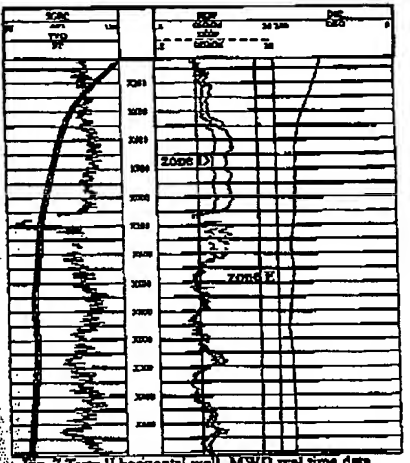

Fig. 7 Type II horizontal well, MWD real time data
Gap in data due to casing

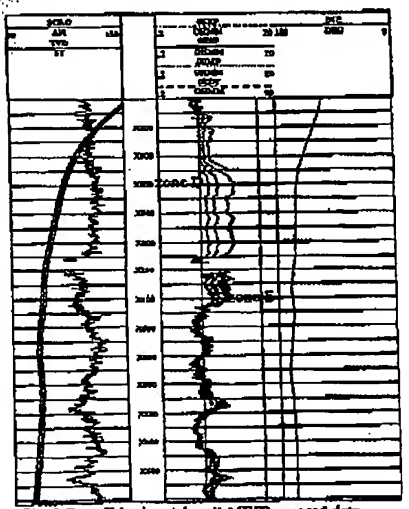

Fig. 8 Type II horizontal well MWD recorad data
Gap in data due to casing

Table 1. Data Table of phase resistivities at various relative dip angles.

FIELD	WELL TYPE	RDA	SESP	SESP	SEMP	SEDP	APPROX TVD	LITHOLOGY	DEPENV	AGE
A	I	62	0.60	0.60	0.70	0.70	4900	SHALE	SHELF	PLIOCENE
A	I	65	0.62	0.55	0.61	0.61	4900	SHALE	SHELF	PLIOCENE
A	I	75	0.72	0.9	0.9	0.9	4900	SHALE	SHELF	PLIOCENE
A	I	62	0.60	0.65	0.60	0.60	4900	SHALE	SHELF	PLIOCENE
A	I	65	0.62	0.68	0.68	0.60	4900	SHALE	SHELF	PLIOCENE
A	I	75	0.60	0.70	0.70	0.70	4900	SHALE	SHELF	PLIOCENE
A	I	62	1.70	1.70	4.80	4.80	4950	SAND	SHELF	PLIOCENE
A	I	65	1.80	1.80	2.40	2.80	4950	SAND	SHELF	PLIOCENE
A	I	75	3.50	10.00	80.00	80.00	4950	SAND	SHELF	PLIOCENE
A	I	80	2.40	8.00	8.00	5.50	4950	SAND	SHELF	PLIOCENE
B	II	0	0.70	0.70	0.80	0.80	7520	SHALE	DELTA FRONT	UPPER MIOCENE
B	II	62	0.90	1.00	1.10	1.10	7520	SHALE	DELTA FRONT	UPPER MIOCENE
B	II	71	1.00	1.10	1.60	1.50	7520	SHALE	DELTA FRONT	UPPER MIOCENE
B	II	83	1.20	1.60	2.60	2.60	7520	SHALE	DELTA FRONT	UPPER MIOCENE
B	II	94	1.40	2.00	3.60	3.60	7520	SHALE	DELTA FRONT	UPPER MIOCENE
B	II	95	1.30	1.90	3.20	3.20	7520	SHALE	DELTA FRONT	UPPER MIOCENE
C	I	45	0.62	0.70	0.80	0.80	9300	SHALE	DELTA FRONT	PLIOCENE
C	I	68	0.97	1.05	1.10	1.10	9300	SHALE	DELTA FRONT	PLIOCENE
C	I	45	9.80	20.00	25.00	30.00	9250	SAND	DELTA FRONT	PLIOCENE
C	I	68	14.00	20.00	50.00	100.00	9250	SAND	DELTA FRONT	PLIOCENE
C	I	45	7.00	15.00	18.00	24.00	9250	SAND	DELTA FRONT	PLIOCENE
C	I	68	15.00	21.00	27.00	27.00	9250	SAND	DELTA FRONT	PLIOCENE
C	I	45	2.00	2.30	3.70	3.70	9315	SAND	DELTA FRONT	PLIOCENE
C	I	68	8.00	20.00	2000.00	2000.00	9315	SAND	DELTA FRONT	PLIOCENE
C	I	45	1.10	1.40	1.70	1.70	9315	SAND	DELTA FRONT	PLIOCENE
C	I	97	3.20	12.00	2000.00	2000.00	9315	SAND	DELTA FRONT	PLIOCENE
D	I	60	1.80	1.90	2.00	2.00	12500	SHALE	UPPER SLOPE	PLIOCENE
D	I	98	13.00	14.00	17.00	17.50	12500	SAND	UPPER SLOPE	PLIOCENE
E	II	0	0.80	0.80	0.90	0.90	8000	SHALE	SHALLOW MARINE	UPPER MIOCENE
E	II	90	0.90	1.00	1.20	1.20	8000	SHALE	SHALLOW MARINE	UPPER MIOCENE
E	II	95	0.90	1.00	1.10	1.10	8000	SHALE	SHALLOW MARINE	UPPER MIOCENE
E	II	70	1.00	1.20	1.30	1.30	8000	SHALE	SHALLOW MARINE	UPPER MIOCENE
E	II	75	1.20	1.70	2.10	2.10	8000	SHALE	SHALLOW MARINE	UPPER MIOCENE
E	II	85	1.90	2.80	6.00	6.00	8000	SHALE	SHALLOW MARINE	UPPER MIOCENE
E	II	80	1.90	2.70	4.60	4.60	8000	SHALE	SHALLOW MARINE	UPPER MIOCENE
F	II	0	0.80	0.80	0.80	0.80	9500	SHALE	SHALLOW MARINE	UPPER MIOCENE
F	II	40	1.00	1.00	1.10	1.10	9500	SHALE	SHALLOW MARINE	UPPER MIOCENE
F	II	60	1.60	1.80	2.00	2.00	9700	SHALE	SHALLOW MARINE	UPPER MIOCENE
F	II	75	1.80	2.10	3.20	3.20	9800	SHALE	SHALLOW MARINE	UPPER MIOCENE
G	II	0	0.80	0.80	0.80	0.80	7800	SHALE	DELTAIC	UPPER MIOCENE
G	II	0	0.80	0.80	0.80	0.80	10440	SHALE	DELTAIC	UPPER MIOCENE
G	II	0	0.80	0.80	0.80	0.80	10800	SHALE	DELTAIC	UPPER MIOCENE
G	II	0	0.80	0.80	0.80	0.80	7800	SHALE	DELTAIC	UPPER MIOCENE
G	II	45	1.90	1.90	1.80	1.90	10440	SHALE	DELTAIC	UPPER MIOCENE
G	II	75	1.80	1.90	2.60	2.60	10830	SHALE	DELTAIC	UPPER MIOCENE